Extended Abstracts of the 1994 International Conference on Solid State Devices and Materials, Yokohama, 1994, pp. 524-526

Successful Hydrogenation Using Furnace-Annealing for High Quality Poly-Si TFTs

Masamichi Okamura, Seiiti Shirai, and Tadashi Serikawa

NTT Interdisciplinary Research Laboratories
3-9-11, Midori-cho, Musashino-shi, Tokyo 180, Japan

Polysilicon thin film transistors are successfully hydrogenated by using furnace-annealing in hydrogen ambient after fabrication. Characteristics of poly-Si TFTs fabricated from either furnace-crystallized poly-Si films or laser-crystallized poly-Si films are significantly improved by this simple method. This hydrogenation technique increases production throughput, and is simpler than conventional plasma-hydrogenation.

1. Introduction

In obtaining high performance poly-Si TFTs, hydrogen passivation (hydrogenation), which terminates defects located in the grain boundaries of poly-Si films and/or the interface of Si/SiO_2, is important as well as formation of high quality poly-Si films and gate SiO_2 films.[1] Hydrogen plasma annealing has been commonly used for hydrogenation;[2-6] however, the throughput of this method is quite low. This is a crucial problem when hydrogenation is used in mass production. To improve the throughput, we have investigated several methods of hydrogenation. In this paper, furnace annealing in hydrogen ambient, called furnace hydrogenation is shown to significantly improve the characteristics of poly-Si TFTs. To the authors' knowledge, this is the first report of a systematical study of furnace hydrogenation.

2. Experimental

Figure 1 shows a cross-section of the coplanar poly-Si TFT structure used in this study. The channel polysilicon films were prepared by two methods: laser-crystallization of Si films deposited by sputtering, and furnace-crystallization of Si films deposited by LPCVD. After definition of silicon islands, a 100-nm-thick gate insulator of SiO_2 film was deposited by sputtering in $Ar\text{-}O_2$ mixed ambient.[7] The gate electrode was a 450-nm-thick phosphorus-doped poly-Si film deposited by LPCVD. Source and drain regions were formed by self-aligned phosphorus implantation. After the SiO_2 isolation film and Al electrodes were formed, furnace hydrogenation was performed in $H_2\text{-}N_2$ mixed ambient at 400 and 430°C, for 20 to 60 min. A different set of poly-Si TFTs were plasma hydrogenated for comparison at 400°C for 5 hours before contact holes and Al electrodes were formed.

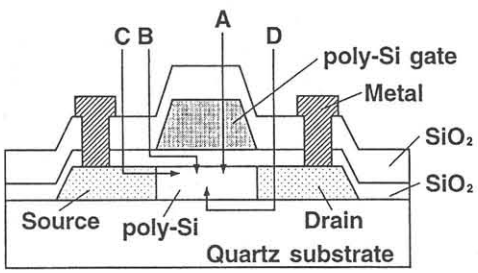

Fig. 1. Cross-section of coplanar poly-Si TFT structure and possible pathways of hydrogen diffusion.

3. Results and Discussions

$I_d\text{-}V_g$ characteristics of the poly-Si TFTs before and after furnace hydrogenation are shown in Fig. 2. Here, furnace hydrogenation was done at 400°C for 20 min. The channel length and width of these TFTs were 20 and 10 μm. All the characteristic features, such as on-current (I_{on}), on/off ratio (I_{on}/I_{off}), threshold voltage (V_{th}) and subthreshold slope (dI_d/dV_g), were significantly improved after furnace hydrogenation for both TFTs fabricated from either furnace-crystallized poly-

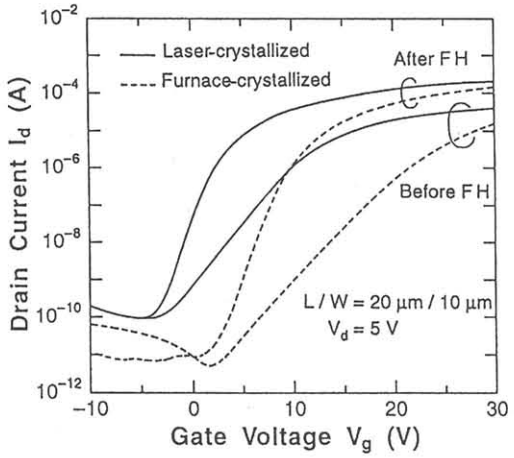

Fig. 2. I_d-V_g characteristics before and after furnace hydrogenation (FH).

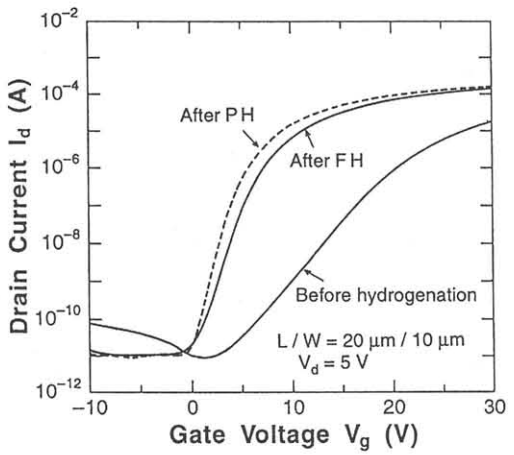

Fig. 3. Id-Vg characteristics of poly-Si TFTs hydrogenated by using furnace hydrogenation (FH) and plasma hydrogenation (PH).

Si films or laser-crystallized poly-Si films.

Figure 3 compares I_d-V_g characteristics of furnace-crystallized poly-Si TFTs hydrogenated by using furnace hydrogenation and plasma hydrogenation. Furnace hydrogenation was performed at 430°C for 20 min. The same effective electron mobility of about 100 cm^2/Vs was obtained for both TFTs. The threshold voltage of the TFT hydrogenated by furnace hydrogenation was slightly higher than that of the TFT hydrogenated by plasma hydrogenation. Furnace hydrogenation at 400°C for more than 60 min resulted in a lower threshold voltage than the threshold voltage shown in this figure. Therefore, the same threshold voltage as obtained by using plasma hydrogenation may be obtained by optimizing the furnace hydrogenation conditions. Some of the TFTs fabricated from laser-crystallized poly-Si films showed a maximum effective electron mobility of about 380 cm^2/Vs after

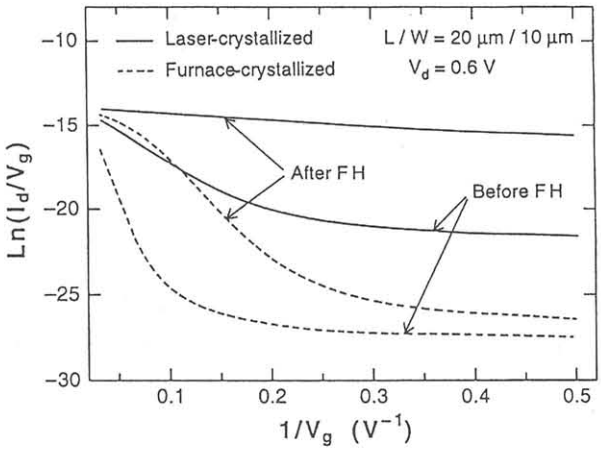

Fig. 4. ln (I_d/V_g) vs. V_g^{-1} plots for obtaining carrier trap state density N_{st} at grain boundaries.

furnace hydrogenation.

Figure 4 plots $\ln(I_d/V_g)$ - V_g^{-1} curves before and after furnace hydrogenation. Slopes of these curves at the small V_g^{-1} indicate carrier trap-state densities (N_{st}) at the grain boundaries.[8] Carrier trap-state densities are significantly reduced to $1.3x10^{12}$ and $4.4x10^{12}$ cm^{-2} after furnace hydrogenation, for laser-crystallized TFTs and furnace-crystallized TFTs, respectively. These values were $3.2x10^{12}$ and $6.7x10^{12}$ before furnace hydrogenation. This is because the dangling bonds at the grain boundaries were effectively terminated by hydrogen atoms and/or molecules by furnace hydrogenation. This implies that the ambience of active atomic hydrogen is not necessary for hydrogenation.

Figure 5 shows threshold voltages of poly-Si TFTs as a function of channel length before and after furnace hydrogenation. The channel widths of the poly-Si TFTs in this figure were 10 and 20 μm. Threshold voltages were significantly reduced by furnace hydrogenation. The threshold voltages of the furnace-crystallized poly-Si TFTs were reduced from about 20 V to about 8.5 V, and those of the laser-crystallized poly-Si TFTs were reduced from about 6 V to about 0 V. Note that changes in threshold voltages are independent of channel length for both channel widths.

There are several possible pathways for hydrogen atoms and/or molecules to migrate to the channel region of poly-Si films and poly-Si/gate-SiO_2 interfaces, as shown in Fig. 1.[4-6] Path A is through the poly-Si gate electrode and the SiO_2 gate insulator, path B involves rapid lateral diffusion in the SiO_2 gate insulator along the channel, path C involves lateral diffusion in the channel poly-Si from the source and drain regions, and path D is through the quartz substrate. To determine which path is dominant, we also

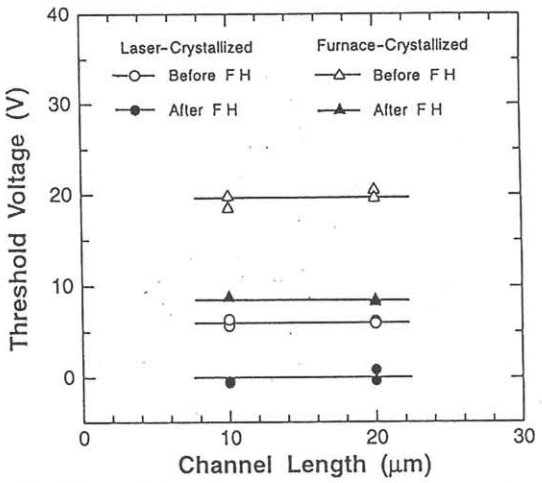

Fig. 5. Channel length dependence of threshold voltages of poly-Si TFTs with channel widths of 10 and 20 μm before and after furnace hydrogenation (FH).

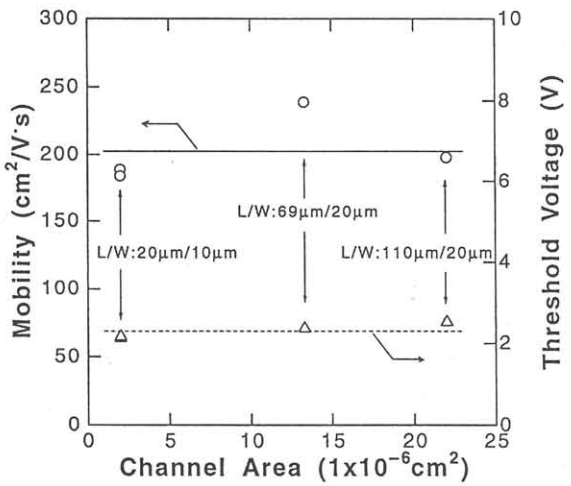

Fig. 6. Channel area dependence of mobilities and threshold voltages of laser-crystallized poly-Si TFTs after furnace hydrogenation.

tested poly-Si TFTs with various channel lengths and widths ranging from 2 to 100 μm.

Figure 6 indicates the channel area (=LxW) dependence of effective electron mobilities and threshold voltages of laser-crystallized poly-Si TFTs after furnace hydrogenation at 400°C for 20 min. Threshold voltages are independent of the channel area. Although relatively large fluctuation is observed, it seems that effective electron mobilities also have no dependence on the channel area. The TFT with a 2μm-long-channel also showed almost the same threshold voltage and effective electron mobility. Excellent characteristics can be obtained for all the poly-Si TFTs independent of their channel lengths and widths. This implies that hydrogen diffusion path A is very important in our case, in addition to the other paths. Therefore, furnace hydrogenation has excellent potential for high-quality poly-Si TFT production because it can effectively passivate poly-Si TFTs of various sizes at a high throughput.

4. Conclusion

We have proposed and developed a very simple hydrogenation process using furnace annealing for high-quality poly-Si TFTs. Experiments demonstrated that excellent characteristics were successfully obtained by using this hydrogenation method for poly-Si TFTs fabricated from laser-crystallized and furnace-crystallized poly-Si films. This hydrogenation method has the advantages of high production throughput and simplicity.

References

1) For example, K. Shimizu, O. Sugiura, and M. Matsumura, IEEE Trans. Electron Devices, 40 (1993) 112.
2) T. I. Kamins, and P. J. Marcoux, IEEE Electron Device Lett., EDL-1 (1980) 159.
3) I-W. Wu, A. G. Lewis, T. Y. Huang, and A. Chiang, IEEE Electron Device Lett., EDL-10 (1989) 123.
4) U. Mitra, B. Rossi, and B. Khan, J. Electrochem. Soc., 138 (1991) 3420.
5) W. B. Jackson, N. M. Johnson, C. C. Tsai, I-W. Wu, A. Chiang, and D. Smith, Appl. Phys. Lett., 61 (1992) 1670.
6) Y. S. Kim, K. Y. Choi, S. K. Lee, B. H. Min, Y. H. Kim, and M. K. Han, *Extended Abstract of the 1993 International Conference on Solid State Devices and Materials*, Makuhari (1993) 443.
7) S. Suyama, A. Okamoto, S. Shirai, and T. Serikawa, Material Research Symp. Proc., 146 (1989) 301.
8) J. Levinson, F. R. Shepherd, P. J. Scanlon, W. D. Westwood, G. Este, and M. Rider, J. Appl. Phys. 46 (1982) 1193.